H-T phase diagram of solid oxygen

T. Nomura,[1,2,*] Y. H. Matsuda,[1,†] and T. C. Kobayashi[3]
[1]*Institute for Solid State Physics, University of Tokyo, Kashiwa, Chiba 277-8581, Japan*
[2]*Hochfeld-Magnetlabor Dresden (HLD-EMFL), Helmholtz-Zentrum Dresden-Rossendorf, D-01314 Dresden, Germany*
[3]*Department of Physics, Okayama University, Okayama 700-8530, Japan*
(Received 4 June 2017; published 25 August 2017)

The comprehensive magnetic field–temperature (H-T) phase diagram of solid oxygen including the θ phase is discussed in the context of the ultrahigh-field measurement and the magnetocaloric effect (MCE) measurement. The problems originating from the short duration of the pulse field, nonequilibrium conditions and MCEs, are pointed out and dealt with. The obtained phase diagram manifests the entropy relation between the phases as $S_\theta \sim S_\alpha < S_\beta \ll S_\gamma$.

DOI: 10.1103/PhysRevB.96.054439

I. INTRODUCTION

In the family of elemental solids, solid oxygen shows characteristic properties due to the magnetic moment of O_2 [1–3]. The exchange interaction between O_2 molecules contributes to condensation energy in addition to the van der Waals interaction. The strength of the exchange interaction greatly depends on the alignment of O_2 molecules [4–7], indicating that the packing structure of solid oxygen is tuned by its magnetic ground state. Moreover, solid oxygen is the only antiferromagnetic (AFM) insulator composed of a single element [8]. Thus, the phase diagram of solid oxygen is a unique playground for testing magnetism in an elemental solid.

In ambient pressure, three phases of solid oxygen appear, γ (54.4–43.8 K), β (43.8–23.9 K), and α (below 23.9 K) [3]. The γ phase is a cubic phase ($Pm\bar{3}n$) where the molecules are rotating at each site. This plastic phase is characterized by large entropy originating from the molecular rotation. The β phase is a rhombohedral phase ($R\bar{3}m$) where the molecular axis is ordered along c direction. It is noteworthy that the entropy difference between the two phases ($S_{\beta\gamma} = 2.04R$, R is the gas constant) is larger than melting [9]. In the β phase, long-range AFM order is suppressed by the geometrical frustration [10]. The α phase is a monoclinic phase ($C2/m$), where the long-range AFM order is realized with lattice deformation.

Recently, an ultrahigh-field phase of solid oxygen, the θ phase, was discovered at around 120 T by using a single-turn coil (STC) [11,12]. The mechanism of the α-θ phase transition is explained in analogy with the O_2-O_2 dimer, as follows. In zero field, the most stable alignment of the O_2-O_2 dimer is the H geometry where two molecules align rectangular-parallel [4–7]. The stability of the H geometry is owing to the maximized π orbital overlapping of the dimer, leading to larger AFM interaction. However, when the magnetization of the dimer is saturated by an external field, AFM interaction is no longer favored and the molecules struggle to decrease it. For instance, if the molecules align in the X geometry (crossed), the overlap integral becomes zero due to the orthogonal geometry [4–7]. Namely, the O_2-O_2 dimer can tune the exchange interaction by changing its alignment. When the strong magnetic field is applied to solid oxygen, it is natural to change the packing structure for smaller AFM interaction. Recently, first-principles calculations have also supported that the canted molecular alignment should be realized in the θ phase (cubic, $Pa\bar{3}$) [13].

The thermodynamical H-T phase diagram of solid oxygen including the θ phase has not yet been clarified. The biggest obstacle is the requirement of the ultrahigh magnetic field above 100 T. Such a high field is generated only by using the destructive pulse technique [14]. Because of the short duration of the field, the phase transition occurs with large hysteresis indicating nonequilibrium conditions [11,12]. In addition, the temperature of the sample could change by the magnetocaloric effect (MCE) during the adiabatic magnetization [15,16]. To obtain the thermodynamical phase boundary, these problems have to be dealt with.

In this paper, the thermodynamical H-T phase diagram of solid oxygen is summarized as a compilation of the experimental works: STC [11,12,15] and adiabatic MCE [16]. In Sec. II, three major problems, (i) nonequilibrium, (ii) irreversible MCE, and (iii) reversible MCE, are explained with results. In Sec. III, sweep-speed dependence of the transition field is classified as a guide for dealing with the problems. In Sec. IV, the H-T phase diagram is carefully constructed with avoiding the problems. We discuss the entropy relation between the phases in terms of the obtained phase diagram. In Sec. V, the conclusion is stated.

II. RESULTS OF THE FIELD-INDUCED PHASE TRANSITIONS

A. α-θ and β-θ transitions in STC

The θ phase has been confirmed by magnetization and magneto-optical measurements [11,12]. Representative results of the α-θ phase transition are shown in Fig. 1. The initial temperature T_0, measured immediately before applying the field, and maximum field strength H_{max} are shown for each curve. The phase transition was observed in the temperature range of $4 < T_0 < 42$ K. At the transition, the rapid increases of magnetization M [Fig. 1(a)] and transmitted-light intensity I [Fig. 1(b)] are observed. The transition fields in up and down sweeps (H_c^+, H_c^-) are shown by the arrows. As increasing H_{max}, hysteresis becomes larger since the phase transition

*t.nomura@hzdr.de
†ymatsuda@issp.u-tokyo.ac.jp

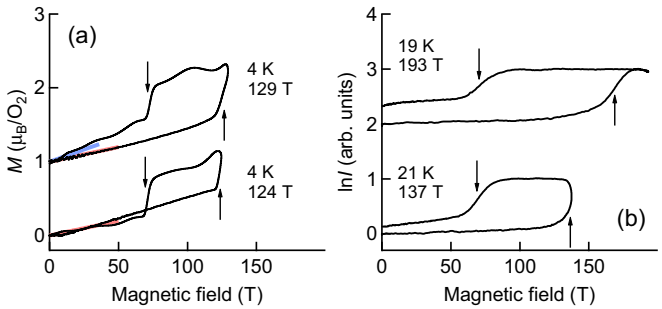

FIG. 1. Results of the STC [11,12]; (a) magnetization and (b) optical measurements. The magnetization curves of the α (red) and β (blue) phases are shown for comparison [2]. The transmitted-light intensity is normalized for letting the change of $\ln I$ be 1. Upward (downward) arrows indicate H_c^+ (H_c^-). Curves are shifted for clarity.

cannot follow the faster sweep of the pulsed field. As a result, H_c^+ and H_c^- are not uniquely defined even at the same T_0. This is problem (i), the effect of nonequilibrium. If we naively plot H_c^+ and H_c^- as a function of T_0, the H-T phase diagram is obtained with large deviation as in Fig. 4(a). In particular, the effect of nonequilibrium is serious in H_c^+.

In Fig. 1(a), the down sweep of the magnetization curve ($H_{max} = 129$ T, $T_0 = 4$ K) accords with the β phase despite that the initial phase is α [2]. This is due to the irreversible heating during the α-θ phase transition [15]. Dissipation related to the first-order phase transition (hysteresis loss and dissipative motion of domain walls) results in the heating effect. Namely, T differs from T_0 after the θ phase appears. This is problem (ii), irreversible MCE. Fortunately, the irreversible MCE is relevant only when H_{max} is relatively higher since it is proportional to the amount of the induced θ phase. The change of T is not significant if the phase transition barely occurs like in the condition of $H_{max} = 124$ T where the down sweep of the magnetization accords with the α phase.

B. β-γ and α-β transitions observed in MCE

The β-γ and α-β transitions have been observed with the adiabatic MCE measurement [16]. Figure 2 shows the results near the (a) β-γ and (b) α-β phase boundaries. When these transitions occur in the adiabatic condition, T changes along the phase boundary. Here, entropy stays constant by balancing T and the fractions of the coexisting phases. Since

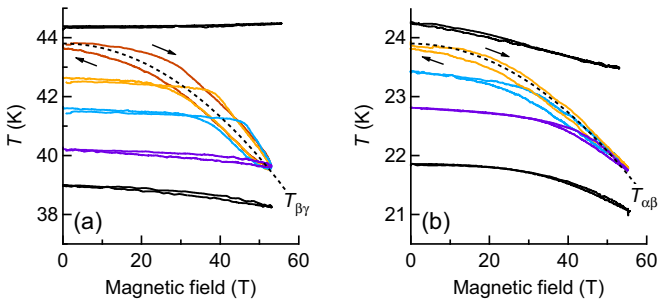

FIG. 2. MCE curves near the (a) β-γ and (b) α-β phase boundaries [16]. H dependencies of the phase boundaries are shown by dotted curves.

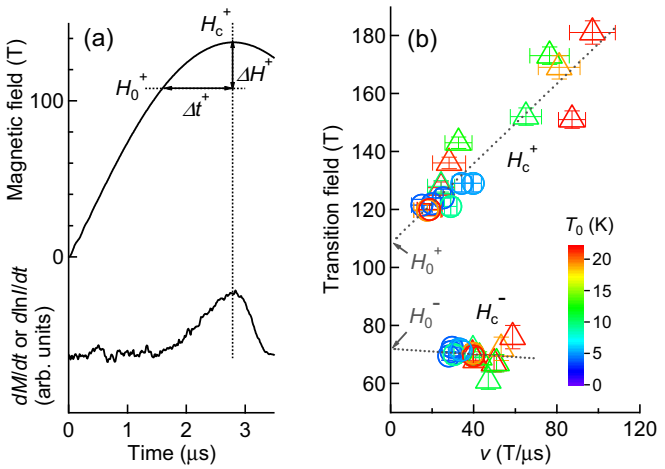

FIG. 3. (a) Graphical definition of the sweep speed $v = \Delta H/\Delta t$. (b) v dependence of the transition field [12]. Circles and triangles show the results of the magnetization and optical measurements, respectively. The color scale shows T_0 for each plot. Dotted line shows the linear fitting of H_c. H_0 is the expected H_c at $v = 0$, and used for the definition of v in the self-consistent way.

the measurement of the STC is adiabatic, T changes from T_0 if the β-γ and α-β phase transitions are induced. This is problem (iii), reversible MCE. The reversible MCE is serious only beneath the β-γ and α-β phase boundaries. If no phase transition occurs, ΔT is less than 1 K even at 50 T [16].

III. SWEEP-SPEED DEPENDENCE OF H_c

We classify the sweep speed v dependence of the transition fields H_c, as a guide for dealing with the problems. In this paper, the superscript + (−) is used for the up (down) sweep. Figure 3(a) shows the definitions of H_c^+ and v^+, which follow the way of Ref. [12]. H_c is defined by the extrema in dM/dt or $d\ln I/dt$. v is self-consistently defined as the averaged sweep speed between the timings at $H = H_0$ and H_c. H_0 is the expected H_c in a quasistatic process [$v = 0$ in Fig. 3(b)]. In this definition, v is obtained as the sweep speed during the phase transition proceeds.

For the α-θ phase transition, H_c is plotted as a function of v in Fig. 3(b). The data at $T_0 < 22$ K are plotted and equally treated since H_c seems to be independent of T_0 in this temperature range. By linear fitting, we obtained the v dependence of H_c as

$$H_c^+ = 0.69(5)\, v^+ + 108(2)\ \text{T}, \tag{1}$$

$$H_c^- = -0.05(6)\, v^- + 72(2)\ \text{T}. \tag{2}$$

By taking the slope 0.69 for up sweep, we correct H_c^+ to the limit of $v = 0$. The corrected transition field H_{c0}^+ corresponds to the value expected at quasiequilibrium conditions. For discussing the thermodynamical phase diagram, H_{c0}^+ is more appropriate since the effect of nonequilibrium is suppressed. In this paper, we apply this correction for all temperature ranges assuming that the β-θ phase transition also follows the same v dependence. For the down sweep, the correction is not applied since B_c^- does not depend on v^- greatly.

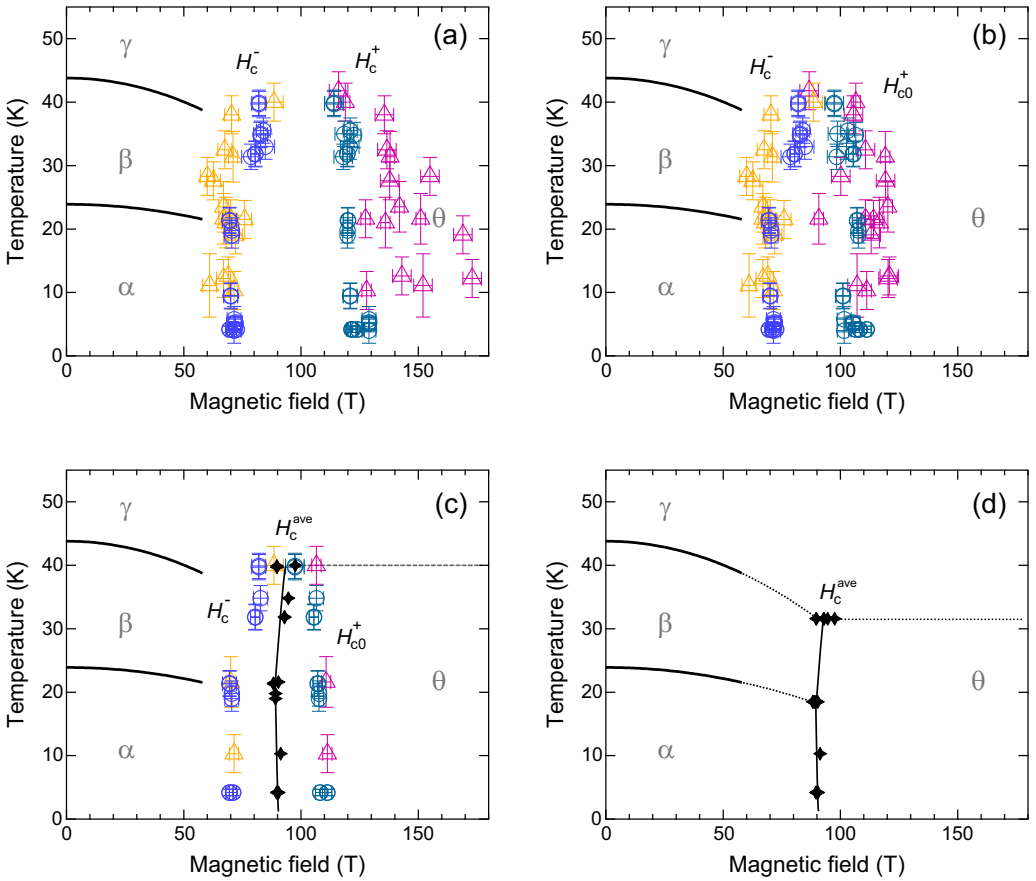

FIG. 4. *H-T* phase diagram of solid oxygen. (a) H_c^+ and H_c^- are plotted as a function of T_0 without any modifications. Circles and triangles show the results of the magnetization and optical measurements, respectively. (b) H_{c0}^+ is plotted instead of H_c^+. (c) The data plots obtained in slower sweep speed ($15 < v^+ < 30$ T/μs) are selected. The averaged transition field $H_c^{ave} = (H_{c0}^+ + H_c^-)/2$ is plotted with black stars with the guiding curve. The gray dashed line is the θ-γ phase boundary expected from the entropy relation. (d) Proposed *H-T* phase diagram of solid oxygen. The reversible MCEs along the β-γ and α-β phase boundaries are taken into account.

IV. PHASE DIAGRAM

In this section, the *H-T* phase diagram is corrected from Fig. 4(a)–4(d) by dealing with the problems one by one. Figure 4(a) is the naively obtained phase diagram, where H_c^+ and H_c^- are plotted as a function of T_0. The β-γ and α-β phase boundaries obtained by the adiabatic MCE measurement are shown by solid curves [16]. Deviation of H_c^+ is due to the nonequilibrium of the α-θ and β-θ phase transitions [11,12]. The v dependence of H_c^+ has to be taken into account for further discussions.

Figure 4(b) shows the corrected phase diagram plotting H_{c0}^+ instead of H_c^+. By the correction, the deviation originating from the problem (i) is greatly suppressed. For discussing the thermodynamical phase diagram, it is usual to read the center of hysteresis as $H_c^{ave} = (H_{c0}^+ + H_c^-)/2$. However, we should be careful because of the temperature change after the field-induced phase transition. Especially after the α-θ phase transition, irreversible heating by as much as 700 J/mol related to the hysteresis loss was observed [15].

To avoid the effect of irreversible MCE [problem (ii)], data plots obtained only with slower v ($15 < v^+ < 30$ T/μs) are selected in Fig. 4(c). Slower v implies that the phase transition barely occurs at the top of the field. Irreversible MCE is considered to be proportional to the fraction of the field-induced θ phase. Therefore, the temperature difference between the up and down sweeps is greatly reduced in this condition. The averaged transition field H_c^{ave} is plotted with black stars. The Clausius-Clapeyron equation

$$dT_c/dH_c = -\Delta M/\Delta S \tag{3}$$

suggests that the obtained steep phase boundary means large ΔM and small ΔS [12].

Here, we quantitatively discuss the entropy relation between the α, β, γ, and θ phases. The slopes of the phase boundaries are roughly estimated as $5 < |dT/dB|_{\alpha\theta}$, $1 < (dT/dB)_{\beta\theta} < 10$ in units of K/T. The differences of the magnetization are roughly estimated as $\Delta M_{\alpha\theta} = 1.2\mu_B/O_2$ and $\Delta M_{\beta\theta} = 1\mu_B/O_2$ [12]. Here, we assumed that the magnetization of the θ phase is saturated ($M_\theta = 2\mu_B/O_2$). Based on Eq. (3), the entropy differences are obtained as $|\Delta S|_{\alpha\theta} < 0.16R$ and $-0.67R < \Delta S_{\beta\theta} < -0.07R$. At zero field, the entropy relation between the α, β, and γ phases is already known as $S_\alpha < S_\beta \ll S_\gamma$ with the differences of $\Delta S_{\alpha\beta} = 0.47R$ and $\Delta S_{\beta\gamma} = 2.04R$ [9]. Summarizing them, the entropy relation is obtained as $S_\theta \sim S_\alpha < S_\beta \ll S_\gamma$. In the following, we assume the γ phase survives at high fields [18] and discuss how the four phases connect to each other in the *H-T* phase diagram.

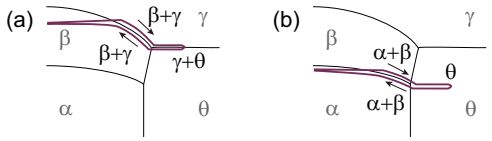

FIG. 5. Expected MCE curves beneath the (a) β-γ and (b) α-β phase boundaries.

Large $\Delta S_{\theta\gamma}$ suggests that the γ-θ phase boundary is flat. In addition, $\Delta M_{\theta\gamma}$ would be almost zero since the magnetizations of the θ and γ phases almost saturate at 150 T. Therefore, the θ-γ phase boundary has to be completely flat as shown by the gray dashed line in Fig. 4(c). Here, the β-γ-θ triple point is not clear since the extrapolated β-γ phase boundary does not smoothly connect to the θ-γ boundary.

For explaining the β-γ-θ triple point, the reversible MCE [problem (iii)] has to be taken into account. The schematic MCE curve is shown in Fig. 5(a). When the magnetic field passes the β-γ phase boundary in the adiabatic condition, T decreases along the phase boundary with increasing the fraction of the γ phase. For example, in the case of $T_0 = 42$ K, 100 T is necessary for the entire phase transition from the β to γ phase [16]. That means the plots beneath the β-γ phase boundary are cooled down to the β-γ-θ triple point with phase coexistence. Finally at the β-γ-θ triple point, the β phase will transform to the θ phase, which is detected in the experiment. At higher field than the triple point, the MCE curve will follow the γ-θ phase boundary with phase coexistence. However, this phase coexistence cannot be confirmed by the magnetization and optical spectroscopy since the γ and θ phases show similar results in these measurements.

The same behavior of MCE would occur also for the α-β phase boundary. Therefore, the data plots around 20 K would also reach to the α-β-θ triple point as shown in Fig. 5(b). At the triple point, the α and β phases wholly transform to the θ phase. When the β-γ and α-β phase transitions are not involved ($T_0 < 15$ K), the effect of the reversible MCE is less than 1 K and negligible [16].

Finally, we propose the H-T phase diagram of solid oxygen as Fig. 4(d). Here, we assume that the data plots around 40 K and 20 K get together at the triple points. The θ-γ transition (solid-plastic transition) is expected to occur at 31 K. This is close to the value of the solid-plastic transition of N_2 (α-β transition, $T_{\alpha\beta} = 35.6$ K) [17].

The thermodynamical α-θ transition field is obtained at around 90 T. Recently, such an ultrahigh magnetic field has become accessible using nondestructive pulse magnets and applied to research in condensed matter physics [19–22]. If the magnetic field is generated for a few ms, $H_{\max} = 100$ T might be enough to observe the θ phase since hysteresis becomes smaller. In this time scale, various kinds of measurement such as magnetostriction, ultrasound, and x-ray diffraction are applicable to obtain the structural information of the θ phase. These measurements are important for revealing the whole picture of the θ phase and for further understanding of oxygen.

V. CONCLUSION

The thermodynamical H-T phase diagram of solid oxygen including the θ phase was proposed as Fig. 4(d). The phase diagram was obtained by analyzing the results of the magnetization, optical, and adiabatic MCE measurements with avoiding the problems originating from the short duration of the field. Using the Clausius-Clapeyron equation, the entropy relation between the phases was obtained as $S_\theta \sim S_\alpha < S_\beta \ll S_\gamma$.

The corrections of the phase diagram applied in Fig. 4 are abstracted as follows. From (a) to (b), H_c^+ was corrected to H_{c0}^+ by using the v dependence of H_c^+ for suppressing the effect of (i) nonequilibrium. From (b) to (c), only the data obtained with slower v were collected for reducing the effect of (ii) irreversible MCE. Here, $H_c^{\rm ave}$ was introduced for discussing the thermodynamical phase boundary. From (c) to (d), the effect of (iii) reversible MCE was taken into account for the consistency of the β-γ-θ triple point. In the adiabatic condition of the STC, T is expected to decrease along the β-γ and α-β phase boundaries and to reach to the triple points.

The ground state of oxygen obviously depends on the external magnetic field since O_2 is a magnetic molecule. The obtained H-T phase diagram will contribute to discussing the thermodynamical stability of oxygen. Potentially, it could lead to controlling the chemical activity of oxygen by magnetic field, during biological reaction or material processing [23,24].

ACKNOWLEDGMENTS

The authors acknowledge S. Takeyama, K. Kindo, A. Matsuo, Y. Kohama, and A. Ikeda for fruitful discussions. T.N. was supported by the Japan Society for the Promotion of Science through the Program for Leading Graduate Schools (MERIT), a Grant-in-Aid for JSPS Fellows, and HLD at HZDR, member of the European Magnetic Field Laboratory. This work was partly supported by JSPS KAKENHI, Grant-in-Aid for Scientific Research (B) (16H04009).

[1] G. C. DeFotis, Phys. Rev. B **23**, 4714 (1981).
[2] C. Uyeda, K. Sugiyama, and M. Date, J. Phys. Soc. Jpn. **54**, 1107 (1985).
[3] Yu. A. Freiman and H. J. Jodl, Phys. Rep. **401**, 1 (2004).
[4] M. C. van Hemert, P. E. S. Wormer, and A. van der Avoird, Phys. Rev. Lett. **51**, 1167 (1983).
[5] B. Bussery and P. E. S. Wormer, J. Chem. Phys. **99**, 1230 (1993).
[6] M. Bartolomei, M. I. Hernández, J. Campos-Martínez, E. Carmona-Novillo, and R. Hernández-Lamoneda, Phys. Chem. Chem. Phys. **10**, 5374 (2008).
[7] M. Obata, M. Nakamura, I. Hamada, and T. Oda, J. Phys. Soc. Jpn. **82**, 093701 (2013).
[8] Yu. A. Freaiman and H. J. Jodl, Low Temp. Phys. **28**, 491 (2002).
[9] W. F. Giauque and H. L. Johnston, J. Am. Chem. Soc. **51**, 2300 (1929).

[10] P. W. Stephens and C. F. Majkrzak, Phys. Rev. B **33**, 1 (1986).
[11] T. Nomura, Y. H. Matsuda, S. Takeyama, A. Matsuo, K. Kindo, J. L. Her, and T. C. Kobayashi, Phys. Rev. Lett. **112**, 247201 (2014).
[12] T. Nomura, Y. H. Matsuda, S. Takeyama, A. Matsuo, K. Kindo, and T. C. Kobayashi, Phys. Rev. B **92**, 064109 (2015).
[13] S. Kasamatsu, T. Kato, and O. Sugino, Phys. Rev. B **95**, 235120 (2017).
[14] N. Miura, T. Osada, and S. Takeyama, J. Low Temp. Phys. **133**, 139 (2003).
[15] T. Nomura, Y. H. Matsuda, S. Takeyama, and T. C. Kobayashi, J. Phys. Soc. Jpn. **85**, 094601 (2016).
[16] T. Nomura, Y. Kohama, Y. H. Matsuda, K. Kindo, and T. C. Kobayashi, Phys. Rev. B **95**, 104420 (2017).
[17] A. Szmyrka-Grzebyk and A. Kowal, Low Temp. Phys. **35**, 329 (2009).
[18] The results of the γ phase at above 100 T were not reproducible. Most probably, it is because of the plasticity; the crystal cracks and moves during the pulsed field.
[19] M. Jaime, R. Daou, S. A. Crooker, F. Weickert, A. Uchida, A. E. Feiguin, C. D. Batista, H. A. Dabkowska, and B. D. Gaulin, Proc. Natl. Acad. Sci. USA **109**, 12404 (2012).
[20] M. M. Altarawneh, G.-W. Chern, N. Harrison, C. D. Batista, A. Uchida, M. Jaime, D. G. Rickel, S. A. Crooker, C. H. Mielke, J. B. Betts, J. F. Mitchell, and M. J. R. Hoch, Phys. Rev. Lett. **109**, 037201 (2012).
[21] J. W. Kim, S. Artyukhin, E. D. Mun, M. Jaime, N. Harrison, A. Hansen, J. J. Yang, Y. S. Oh, D. Vanderbilt, V. S. Zapf, and S.-W. Cheong, Phys. Rev. Lett. **115**, 137201 (2015).
[22] S. Zherlitsyn, V. Tsurkan, A. A. Zvyagin, S. Yasin, S. Erfanifam, R. Beyer, M. Naumann, E. Green, J. Wosnitza, and A. Loidl, Phys. Rev. B **91**, 060406(R) (2015).
[23] M. Kurahashi and Y. Yamauchi, Phys. Rev. Lett. **114**, 016101 (2015).
[24] K. Kitazawa, Y. Ikezoe, H. Uetake, and N. Hirota, Physica B. **294-295**, 709 (2001).